Vehicle System Dynamics
Vol. 00, No. XX, XXX 20XX, 1–24

Advanced Emergency Braking under Split Friction Conditions & the Influence of a Destabilising Steering Wheel Torque

Kristoffer Tagesson[a†] and David Cole[b]

[a]*Division of Vehicle Engineering & Autonomous Systems, Chalmers University of Technology, and Department of Chassis Strategies & Vehicle Analysis, Volvo Group Trucks Technology, Gropegårdsgatan, SE-405 08 Göteborg, Sweden*
[b]*Department of Engineering, University of Cambridge, Trumpington Street, Cambridge CB2 1PZ, UK*

(*Received 00 Month 200x; final version received 00 Month 200x*)

The steering system in most heavy trucks is such that it causes a destabilising steering wheel torque when braking on split friction, that is, different friction levels on the two sides of the vehicle. Moreover, advanced emergency braking systems are now mandatory in most heavy trucks, making vehicle induced split friction braking possible. This imposes higher demands on understanding how the destabilising steering wheel torque affects the driver, which is the focus here. Firstly, an experiment has been carried out involving 24 subjects all driving a truck where automatic split friction braking was emulated. Secondly, an existing driver-vehicle model has been adapted and implemented to improve understanding of the observed outcome. A common conclusion drawn, after analysing results, is that the destabilising steering wheel torque only has a small effect on the motion of the vehicle. The underlying reason is a relatively slow ramp up of the disturbance in comparison to the observed cognitive delay amongst subjects; also the magnitude is low and initially suppressed by passive driver properties.

Keywords: heavy vehicles; braking; steering; steering torque; driver model; neuromuscular;

1. Introduction

Advanced emergency braking, also known as autonomous emergency braking, has been identified as a very promising technique to reduce the number of accidents in traffic [1, 2]. In Europe this has been taken one step further as an advanced emergency braking system, AEBS, is mandatory in a majority of heavy trucks, from November 2015 [3]. In practice this means that new trucks should be equipped with sensors to detect a potential collision and automatically activate brakes when the driver fails to do so. The system should however not activate 'in situations where the driver would not recognise an impending forward collision', see [3]. That is, warning or heavy braking must not be activated too early. This condition requires that the action of the emergency brakes is heavy in order to avoid a collision.

The stability of an articulated truck combination during heavy braking was extensively analysed in the 50s, 60s, and 70s [4]. The main instability modes considered were snaking, jack-knifing and trailer swing-out. The work led to the introduction of automatic load dependent brakes and anti-lock braking systems, ABS, and eventually to legal requirements for such systems [5]. Today, many heavy trucks have electronically controlled brakes; this makes it possible to achieve exact brake

†Corresponding author. Email: kristoffer.tagesson@volvo.com

ISSN: 0042-3114 print/ISSN 1744-5159 online

DOI: 10.1080/0042311YYxxxxxxxx
http://www.informaworld.com

distribution and thereby good directional stability in general. There are however yet a few cases where the directional motion of the vehicle combination may be affected upon activation of brakes, here listed:

- When having faulty brakes;
- When cornering close to the limits of friction;
- When driving on a road with uneven limits of friction between left and right vehicle sides, known as split friction or split-μ

Faulty brakes should obviously be covered by proper diagnostics and maintenance. Whereas for the second case, braking in a turn, Morrison and Cebon [6] showed that with a properly designed ABS system it is possible to maintain directional stability yet only cause a marginal increase in braking distance. The final and last case will be the focus of this paper, split-μ braking, and in particular when brakes are triggered by AEBS in a heavy truck.

Common reasons for split-μ are: oil spillage, uneven ice coating, and one-sided aquaplaning. When cruising or braking gently the driver may not even notice the effect, but when braking hard in an emergency situation substantially higher braking forces will act on the high friction side compared to the low friction side. This will cause the vehicle to pull sideways, primarily due to the induced overall yawing torque, and possibly roll-over. Trucks towing one or more trailers also risk jackknifing [7]. In the event of modest rotation the driver can steer and balance uneven braking forces. However if the driver is surprised by the situation and thus is unprepared it is likely that substantial lateral deviation from the intended lane can occur before the driver has responded. This can result in the vehicle running off the road or colliding with oncoming traffic. When brakes are triggered by AEBS, and not by the driver, it can be argued that it is more likely that the response from the driver would be slower. This was analysed in an experiment with twelve volunteers driving a solo truck in [8]. The main conclusion was that the expected lateral deviation, upon AEBS activation on split-μ, for an alert driver is low, but for a distracted driver more support might be required. This assumes a truck combination compliant with the legal requirements stated in [5].

The most straightforward approach to ensure that the vehicle does not leave its intended lane would be to limit the usage of brakes, in a split-μ situation, based on an estimate of the driver's ability to handle the yaw disturbance. A method for this is proposed in [9]. It does however result in a substantially longer stopping distance when the driver is assumed to be passive, as a restrictive approach must apply when using brakes. Ideally this should be accounted for by moving the onset of brakes earlier in time. But when considering that early predictions of upcoming road conditions as well as crash risk are often unreliable it is realised that this can be hard in practice. Therefore to achieve a short stopping distance on split-μ surfaces it does seem necessary to assist the driver in maintaining directional control. Some heavy trucks are equipped with automatic steering also on axles other than the leading one. For these the braking distance could be reduced without requiring more effort from the driver, as exemplified in [10]. For all other heavy trucks that are commercially available today the only interface for steering is via the steering wheel. A significant minority of trucks are specified today with electronic torque overlay actuation [11, 12]; the majority have traditional hydraulic power steering. For this majority the opportunity to actively support the driver via steering is low, but there are several important geometrical settings to tune. One of these, relevant during split-μ braking, is the steering axis offset at ground, also known as kingpin offset at ground, denoted as r_k. This measure is defined in [13] as the distance in the lateral direction between the wheel plane and the point where the steering axis

intersects the ground plane[1]. When the steering axis intersects the ground plane inside the wheel plane r_k is said to be positive and in the opposite case negative.

Due to packaging reasons heavy trucks have positive kingpin offset at ground; this is different from modern cars that have almost zero or slightly negative offset. When there is a difference in the longitudinal force acting on the two front wheels a positive offset results in a destabilising steering wheel torque, meaning a torque acting on the steering system that acts to turn the vehicle in the same direction as the induced yawing torque. This is the case for example under split-μ braking and also front tyre blow out. In [16] a study was performed to quantify the importance of r_k during tyre blow out. An experiment was run with a solo tractor on a test track including 20 drivers. All were exposed to emulated repetitions of a front tyre blow out, some runs with r_k =12 cm and some with r_k =0 cm. This corresponded to 3 Nm and 0 Nm respectively of steering wheel disturbance. The general conclusion found was that the lateral vehicle deviation was lower when the destabilising steering wheel torque was removed and that this could slightly reduce the number of fatalities caused by tyre blow outs. In the present paper the aim is to quantify the effect of a positive kingpin offset when AEBS is activated on a split-μ surface. Better understanding of the underlying driver and vehicle dynamics during the scenario are also sought.

There are many previously published experimental studies of driver and vehicle response to unexpected transient disturbances or fault conditions. The development of steering technologies such as lane keeping assistance and collision avoidance has partly motivated such studies. One example is the experiment by Switkes et al. [17] who investigated drivers' responses to torque disturbances on the steering wheel. An instrumented vehicle was programmed to generate various shapes (step or ramp) and amplitudes of torque disturbance. Results suggested that there was little difference in the responses of younger and older drivers. The response of the driver to step disturbances was faster than to ramp disturbances.

Despite these previous studies, none appears to have analysed in detail the effects of a destabilising steering wheel torque during automatic split-μ braking of a heavy truck. The objectives of the work described in this paper are to:

- Measure experimentally the lateral path deviation of a tractor unit subjected to unexpected and repeated AEBS split-μ events, for a wider range of drivers (24) than previously investigated [8];
- Deduce the influence of positive kingpin offset on the lateral path deviation of the tractor unit during the AEBS split-μ events. The effect of kingpin offset was previously only investigated for a tyre blow out scenario [16];
- Use a driver-vehicle model [18] incorporating neuromuscular dynamics to aid deeper explanation of the observed behaviour of the driver and vehicle. Such a model has not been used previously for the scenario of a heavy truck in AEBS split-μ events.

The paper is structured as follows: Section 2 describes the details of the experiment; results from this follow in section 3; then section 4 introduces the driver-vehicle model used to explain the fundamental behaviour observed; the corresponding results from simulations are given in section 5; a discussion of the overall results is given in section 6; then section 7 concludes the paper. Notations used comply with ISO 8855, [13], and units are SI unless otherwise stated.

[1]In ISO 8855 [13] r_k is referred to as steering axis offset at ground or kingpin offset at ground; a definition also used in this paper. In [14] it is referred to as kingpin offset at ground or scrub and in [15] as scrub radius. The term scrub radius is differently defined in ISO 8855 [13] as the distance from wheel contact centre to the point where the steering axis intersect ground, i.e. also affected by caster.

2. Experimental Set-up

The experiment involved 24 subjects all driving a solo tractor unit. The tractor unit was configured to perform emulated automatic split-μ braking and the kingpin offset at ground was varied virtually. The test was run in connection with the automatic brake test described in [8] and the tyre blow out test described in [16]. This section will describe the set-up of the test and also what precautions were taken in order to guarantee safety.

2.1. *Test Track*

The test was run on a large brake and handling area marked with a 300 m long and 3.6 m wide straight lane. This provided sufficient safety margins. The temperature was 3-8^{o}C and the track was slightly wet, but it did not rain. The set-up is illustrated in Fig. 1. To discourage drivers crossing the lane markings soft cones were put in the adjacent lanes.

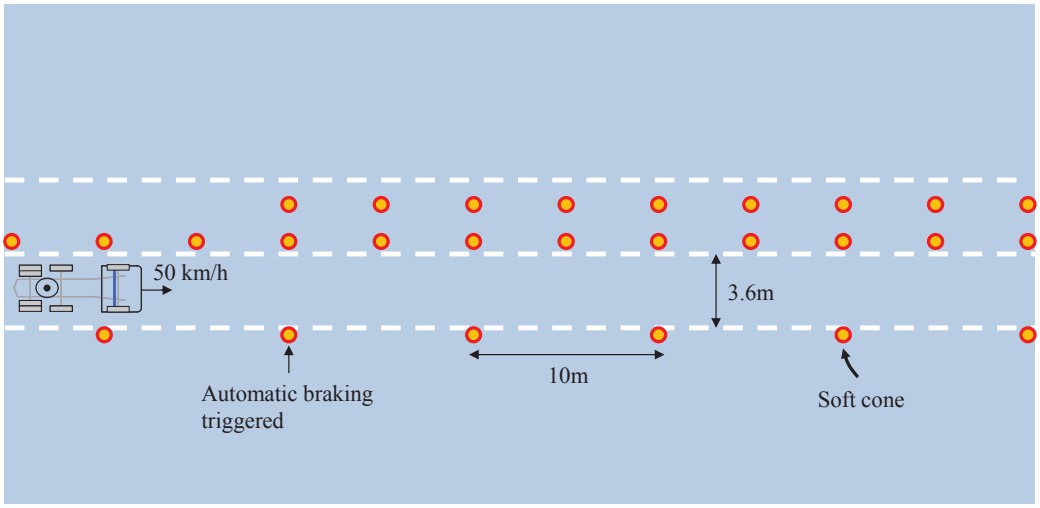

Figure 1.: Test track set-up.

2.2. *Test Vehicle, Controls & Instrumentation*

A solo 6×2 pusher tractor was used in the experiment having the pusher axle (the first rear axle) lifted. The test was performed without a trailer to avoid any risk of jack-knifing. Basic dimensions of the tractor unit are provided in Table 1.

The vehicle was equipped with Volvo Dynamic Steering, which is a column-mounted electric power steering unit. The system contains the ability to fully suppress steering wheel torque disturbances coming from road tyre interaction. Desired terms, owing to vertical and lateral tyre forces, are however maintained by using models of the intended behaviour. This makes the steering system act as a conventional one when having 0 cm of kingpin offset at ground. The system was made configurable also to function as a conventional power steering system with preserved steering torque characteristics, which then is analogous to 12 cm of kingpin offset at ground. The two modes will consequently almost be copies of each other during normal driving, but deviate when braking on split-μ. Since the system removes tyre disturbances in the 0 cm case it will also remove torque components

Table 1.: Specification of Volvo FH tractor used. ©2016 IEEE. Reprinted, with permission, from [16].

Property	**Value**	**Unit**	**Description**
L	4.1	m	Wheelbase, distance between front and drive axle
$F_{z,f}$	58470	N	Front axle vertical load
$F_{z,p}$	0	N	Pusher axle vertical load (lifted)
$F_{z,d}$	29430	N	Drive axle vertical load
i_s	23.2	-	Ratio of steering wheel angle to road wheel angle
r_{StW}	0.225	m	Steering wheel radius, from centre to rim edge

caused by steering system inertia located below the column. In practice this will be of minor importance as there are other more dominant steering torque elements present [19].

Automatic emergency braking on a split-μ surface was emulated by applying more brake action on left side compared to right side of the vehicle while running on a uniform asphalt surface. This was chosen in favour of using a split-μ track because of safety reasons and to avoid test subjects anticipating the vehicle's behaviour. The ratio of left to right brake force was four to one. This ratio was chosen to match the yaw response observed during real split-μ braking using the same truck when running the standard braking system[1]. The standard braking system was compliant with the legal requirements in [5].

A target deceleration of 3.5 m/s^2 was used in the trials; this was derived from two legal requirements on AEBS in [3]. The first one states that a target vehicle travelling in the same direction at 32 km/h shall not be hit when the subject vehicle initially is travelling at 80 km/h. The second one is the earlier mentioned requirement stating that AEBS should 'avoid autonomous braking in situations where the driver would not recognise an impending forward collision'. In [20] a study on truck driver braking behaviour was made based on euroFOT data. At 80 km/h it was observed that brake initiation sometimes occurred as late as time to collision 3.9 s. The deceleration required to reduce vehicle speed from 80 km/h to 32 km/h in 3.9 s is approximately 3.5 m/s^2 and therefore this was the target value used in the trials.

The target was fed into a proportional-integral, PI, acceleration controller with feedforward, see Fig. 2. The measured longitudinal acceleration, $\vec{a}_x$, was input to the controller, which produced the requested total longitudinal force, $\vec{F}_x$. This force was distributed amongst front and drive axle wheels. The relation between brake force left to right was as earlier stated four to one. The relation between brake force front to rear was set in proportion to a corresponding calculated axle load as the vehicle was decelerating at 3.5 m/s^2. Here a centre of gravity height of 1 m was assumed. To go from brake force to brake pressure a linear relation was assumed, more specifically 3.4×10^{-4} Bar/N per wheel which was derived from constant brake pressure tests. The resulting brake pressures P_{fl},P_{fr},P_{rl}, and P_{rr} (with index front/rear,left/right) were applied at the corresponding wheel via the electronically controlled brake system, EBS. The sample rate of the acceleration controller was 100Hz, which was compatible with the rates used in the EBS. The rate was confirmed fast enough to produce repeatable and stable braking. Further

[1]With the standard braking system the observed yaw rate reached about 4 deg/s when pushing the brake pedal to its lowest position on a split-μ track as the steering wheel was held fixed at 0 deg. Entry speed was 40 km/h, the friction coefficient on the low mu side was estimated to 0.1 and 0.6 on the high friction side. A corresponding experiment with the emulated set up is described in section 4.1.

details about the controller are listed in Table 2 along with the parameter values used. In case the driver pressed the brake pedal a select high pressure routine was used per wheel. If the driver pressed the accelerator pedal the test was aborted, this was due to settings in the EBS that were not possible to change.

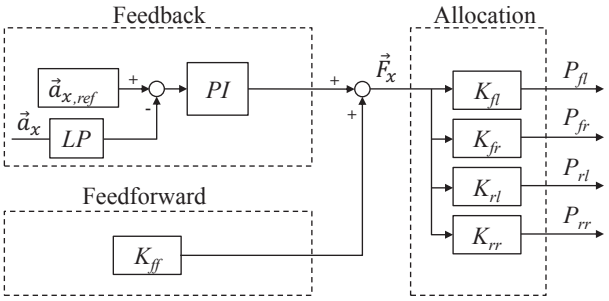

Figure 2.: Brake controller set-up.

Table 2.: Specification of brake controller.

	Notation	Value	Unit
Feedback			
1st order low pass filter (LP) time const.		0.2	s
Target longitudinal acceleration	$\vec{a}_{x,ref}$	-3.5	m/s^2
PI saturation		±6000	N
P-gain		4000	N/m/s^2
I-gain		20000	N/m/s
Integrator saturation		±2000	N
PI activation time		1.5	s
PI error linear ramp up duration		0.5	s
Feedforward			
Braking force	K_{ff}	-18000	N
Allocation			
Allocation constant	K_{fl}	-2.04×10^{-4}	Bar/N
Allocation constant	K_{fr}	-5.10×10^{-5}	Bar/N
Allocation constant	K_{rl}	-6.79×10^{-5}	Bar/N
Allocation constant	K_{rr}	-1.70×10^{-5}	Bar/N

The on-board truck sensors were recorded during the whole test. The sensors included yaw rate, lateral acceleration, steering wheel angle, steering wheel torque, wheel speeds, brake pressure, accelerator pedal position and brake pedal position. A high precision GPS, placed above the drive axle, was also used and recorded.

2.3. *Test Drivers & Test Procedure*

Only professional drivers, normally driving durability tests of trucks, took part. Apart from this no particular criteria were applied when selecting drivers. The average age was 43, the oldest driver was 60 and the youngest 27. Three drivers were female corresponding to 12% (this can be compared to 4% which was the proportion of female truck drivers in Sweden 2013 [21]). Also, a variety of body

proportions were represented. Only one driver had experience from pure brake or handling tests.

Drivers were not aware of the true purpose of the test in order to preserve the effect of surprise. They were instead told that the intention of the test was to record normal positioning in lane and that they should run back and forth inside a straight lane for 300 m. Cruise control was set to 50 km/h. After running back and forth for 5 minutes, without any intervention, an operator fired the automatic braking as described. In this first run half of the drivers were subjected to the steering wheel disturbance and the other half were not, here referred to as group A and B respectively. The basis for forming groups was random. Fig. 3 shows the distribution of age in the two groups. As seen the two groups have nearly the same number of drivers being older and younger than the overall average age. For a complete list of driver age and group membership see Table 5 in Appendix.

The initial exposures were followed by several repetitions according to the order listed in Table 3. Since drivers were completely unaware of the first intervention these runs will in the following be referred to as unexpected, whereas all other runs will be referred to as repeated. The first four runs were all run at 50 km/h. This was considered to be an upper limit not to jeopardize safety. As the drivers were less surprised in the following runs speeds up to 70 km/h were considered as safe. As seen in Table 3 some exposures of emulated front tyre blow out were also incorporated into the experiment; this part has been reported in [16] and will not be treated herein.

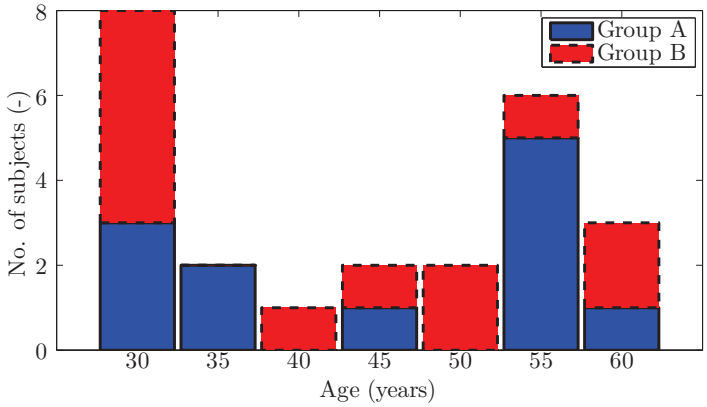

Figure 3.: Distribution of driver age in the two groups.

3. Experimental Results

All 24 initial unexpected exposures where successfully recorded. The trajectories of the truck's centre of gravity in all these 24 runs are shown in Fig. 4(a), with global longitudinal position x_E and lateral position y_E. The curves have been translated so that the coordinate (0,0) m corresponds to where the operator initiated the event. They have also been rotated to produce zero heading, calculated over 0.5 s before activation. The colours red and black are used both here and in the remainder of the paper to represent runs without steering wheel disturbance (r_k=0 cm) and with (r_k=12 cm), respectively. Thin lines correspond to individual runs. Thick lines are the calculated averages of all corresponding valid thin lines, i.e. after removing runs where the driver pressed a pedal.

Table 3.: Test order in experiment where brakes were activated by an operator, with four times more brake action on left side compared to right side of the vehicle, thereby emulating split-μ.

Run	Description	Steering wheel disturbance	
		Group A	Group B
1	Unexpected split-μ braking, 50 km/h	Yes	No
2-4	Repeated split-μ braking, 50 km/h	Yes	No
-	Emulated front tyre blow outs		
5	Repeated split-μ braking, 70 km/h	Yes	No
6-8	Repeated split-μ braking, 50 km/h	No	Yes
-	Emulated front tyre blow outs		
9	Repeated split-μ braking, 70 km/h	No	Yes

Out of the 24 recordings there were two from each group that either pressed the brake or the accelerator pedal during the first 3.5 s (after this time the average speed is below 10 km/h). These four are therefore not included when calculating the average trajectories of the two groups, which are also shown in Fig. 4(a) as two thick lines. Obviously the variability in response is big, ranging from 4 cm to 62 cm in maximum deviation, whereas the observed difference between the average of the two groups is insignificant. Although the extreme values of maximum deviation seen in Fig. 4(a) belong to runs without steering wheel disturbance, there is no significant correlation between (i) the variance of the trajectories from driver to driver and (ii) the presence of absence of steering wheel disturbance.

Now, turning to Fig. 4(b) where all repetitions, run at 50 km/h, are shown. In total there are 100 successfully recorded events of which 73 qualify as valid for calculation of average and other statistical analysis, according to the previously mentioned criteria (for a complete list of valid runs per driver see Table 5 in Appendix). A paired t-test amongst the remaining 16 drivers (8 from each group), who are represented by at least one valid run both with and without steering wheel disturbance, shows that the reduction in maximum lateral deviation when removing the disturbance is 2.4$\pm$7.7 cm (95% confidence interval), which is an insignificant difference. What is more interesting is that there is a small marginally significant difference, immediately after the start of the event up until 10 m of travel. For example, at 9 m of travel the difference is 1.1$\pm$0.9 cm. The root cause of this becomes more clear when looking at Fig. 5, which shows the time series associated with the graphs in Fig. 4. When comparing the steering wheel angle in the repeated case, again using a paired t-test, no difference can be observed. But when doing the same thing for yaw rate a small significant difference appears from the start of the event to around 0.25 s. This suggests that it is merely a coincidence that a small difference appeared in trajectory and that it depends on the initial state of the vehicle and not the steering wheel disturbance. The values from the two t-tests are shown in Fig. 6.

The steering wheel angle response is of course central when considering a steering wheel disturbance, so it deserves some more attention. In [16] where a similar comparison was performed, but instead considering front tyre blow out producing 3 Nm of disturbance and including roughly the same number of subjects, a small overshot was seen caused by the disturbance after 0.3-0.5 s. This is also what could be expected from a destabilising steering wheel disturbance arising from an emergency braking event on a split-μ surface where asymmetric braking force act on the two front wheels. In fact this can be dimly seen also here. On average this

overshot is 3.7^o in the unexpected runs and reduces to about half in the repeated series. An approximate calculation suggests that 3.7^o over 0.2 s would induce 2 cm of deviation in 20 m travel, which might be regarded as an insignificant effect.

The steering wheel torque response, seen in Fig. 5, differs as expected when a disturbance is present compared to when it is not. Without disturbance the torque starts to build up after 0.4-0.5 s due to driver action. Then as the vehicle speed reduces the torque reduces due to increasing power assistance. With disturbance, the torque starts to build up already at time 0.1 s due to split-μ braking forces and kingpin offset. For the repeated runs the two cases differ by at most 2.2 Nm on average, which occurs after 0.42 s. The difference thereafter reduces first to 1.43 Nm, as the steering wheel angle step is completed at time 0.9 s, and later to about 1 Nm.[1]

Another interesting aspect of the data in Fig. 4 and Fig. 5 is how drivers' responses developed with increasing numbers of exposures. Just by comparing the average lines between Fig. 4(a) and Fig. 4(b) it is clear that the lateral deviation is reduced when comparing the unexpected runs to the repeated ones. The same also holds true when comparing the third to the second exposure, and the fourth to the third and so on. The main reason, which one might also expect, is reduced reaction time. For instance, when comparing the average steering wheel angle from recordings in Fig. 5(a) to recordings in Fig. 5(b) the reaction time is in the order of 0.1 s shorter.

The yaw rate response profiles seen in Fig. 5 all show a one period sine wave of frequency 0.7 Hz. This frequency can be in the vicinity of the resonance frequency of several truck combinations in which the motion of the leading unit amplifies as it reaches trailing units. This phenomenon is known as rearward amplification and is described in [22]. At this resonance frequency the lateral deviation and risk of roll-over of the combination is higher than at other frequencies as small excitation of the leading unit can result in high excitation of trailing units. Just like already stressed in [8] it is therefore important to continue with a similar experiment including trailers to analyse if drivers change their steering response or not. And if not, quantify the implied risks.

The runs performed at 70 km/h show very similar results to the repeated 50 km/h runs: almost identical lateral deviation on average with an insignificant difference between runs with and without steering wheel disturbance; the same level of steering wheel torque; the same typical steering wheel angle response, with an insignificant difference between runs with and without steering wheel disturbance; and the same typical yaw rate response.

4. Mathematical Vehicle and Driver Model

This section presents the details of the driver-vehicle model developed to reproduce test runs in simulation. The ultimate purpose has been to gain detailed understanding about the consequences of having a destabilising steering wheel torque.

[1]These levels are all lower than reported in [8] by about 0.5 Nm during the first second. In the present paper all measurements of steering wheel torque are taken from a torsion bar torque sensor located right below the steering wheel. In [8] the same source was used except when the torque disturbance was estimated (in [8] Fig. 5 steering wheel torque, blue dashed line) where it instead was measured right below the electronic power steering unit; this fact was not reported in [8]. The difference of 0.5 Nm is therefore likely due to friction that is acting in-between these two locations. After 1 s the difference tends to be even higher. This can be explained by the fact that the average steering wheel angle happens to differ between the two groups (later shown in Fig. 11 of the present paper). This causes the steering wheel torque arising from lateral and vertical tyre forces to change.

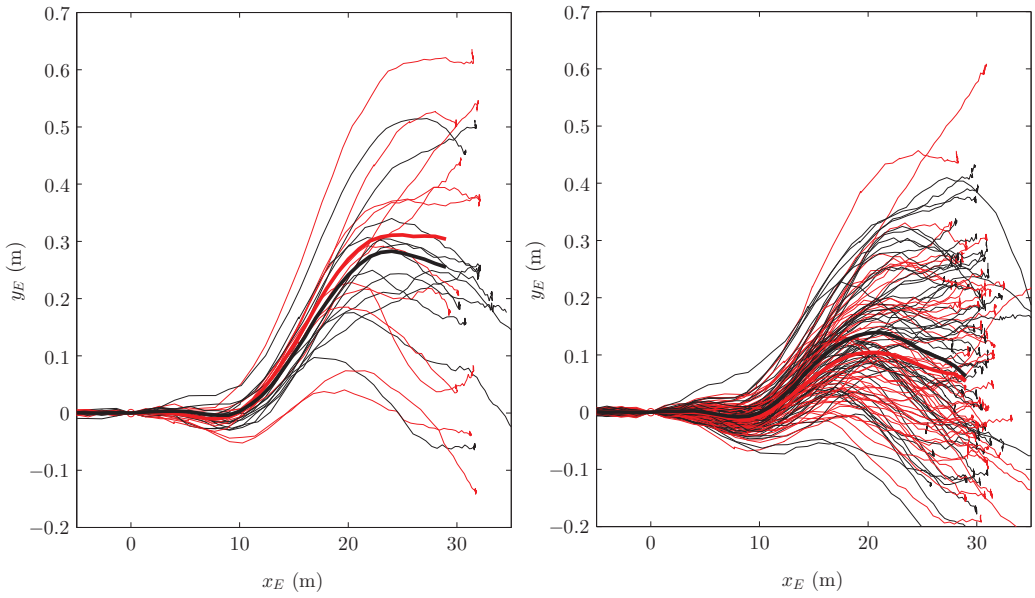

(a) Unexpected runs. (b) Repeated runs.

Figure 4.: Measured trajectories of the truck's centre of gravity, at initial speed 50 km/h. Red and black thin lines correspond to individual runs without and with steering wheel disturbance respectively. Red and black thick lines are the corresponding averages of valid runs without and with disturbance respectively.

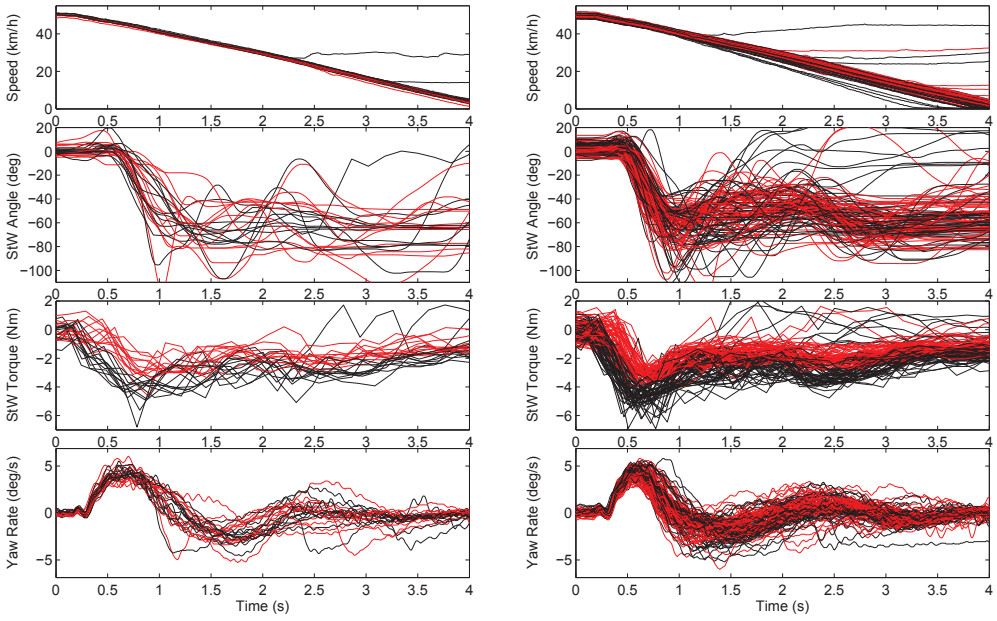

(a) Unexpected runs. (b) Repeated runs.

Figure 5.: Measured time series at initial speed 50 km/h. Red lines correspond to individual runs without steering wheel disturbance. Black thin lines correspond to individual runs with steering wheel disturbance active. StW means steering wheel.

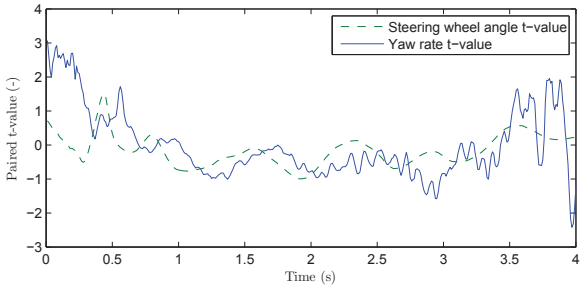

Figure 6.: Paired t-test for repeated runs. In this case 15 degrees of freedom are involved, which makes the 95% confidence level correspond to ±2.13.

The vehicle model contains a linear one track model to represent planar dynamics; vertical, roll and pitch dynamics are not included. It also contains a model of the steering system to simulate the steering wheel torque. The driver model comprises a neuromuscular part representing the dynamics of arms, muscles and the stretch reflex-loop. In addition it also contains a model of the driver's cognitive control actions. The combined driver and vehicle model is shown in Fig. 7. All details and notations seen in the figure are explained throughout the remainder of this section. The values of all parameters are listed in Table 4.

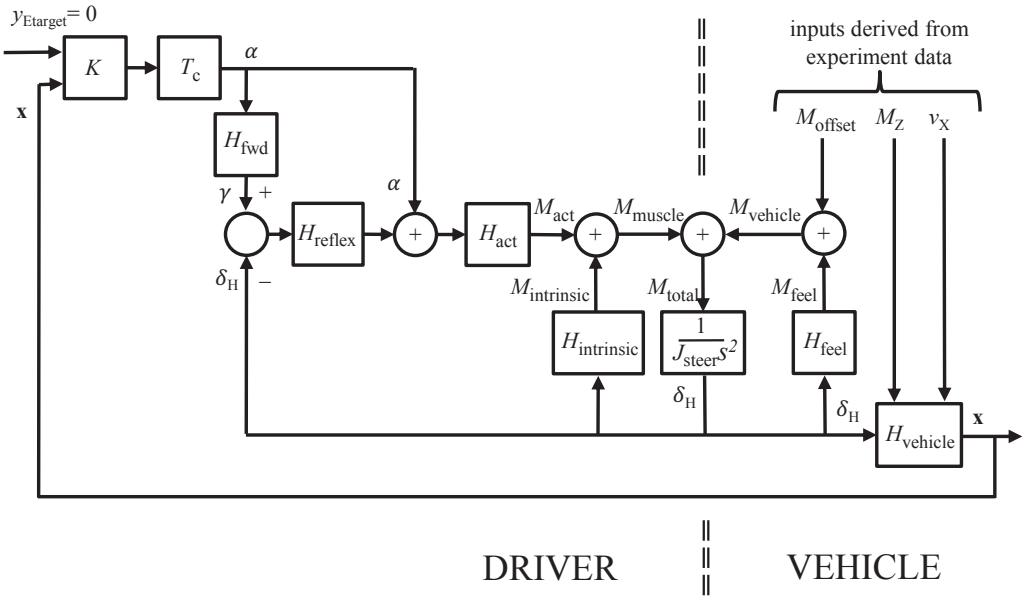

Figure 7.: Block diagram of driver-vehicle model.

4.1. *Vehicle Planar Dynamics*

Fig. 8 provides an illustration of the planar vehicle dynamics model, where m is the mass of the vehicle, v_Y the lateral velocity, ω_Z the yaw rate, v_X the longitudinal velocity, I_Z the yaw inertia, a the longitudinal distance from the centre of gravity to the front axle, b the longitudinal distance from the centre of gravity to the rear axle, M_Z the yaw torque caused by uneven braking, ψ the yaw angle (sometimes referred to as heading), and δ_f is the steer angle of the front axle. The position

Table 4.: Values of parameters in mathematical model (values in brackets are for the repeated runs.)

Property	Value	Unit	Description
Vehicle planar dynamics			
m	8960	kg	Mass
I_Z	25000	kgm^2	Yaw inertia
a	1.373	m	CoG to front axle distance
b	2.727	m	CoG to rear axle distance
C_f	200	kN rad^{-1}	Front axle cornering stiffness
C_r	238	kN rad^{-1}	Rear axle cornering stiffness
d	0.6	m	Brake action distance
Steering system			
i_s	23.2	-	Steering angle ratio
k_s	1.5	Nm rad^{-1}	Steering stiffness
c_s	0.4	Nm s rad^{-1}	Steering damping
v_{ref}	7	m s^{-1}	Reference speed
r_f	0.665	-	Brake balance
r_{split}	0.6	-	Brake split
r_k	0 or 0.12	m	Steering axis offset at ground
p_s	30	-	Power steering torque ratio
J_{mech}	0.05 or 0.09	kgm^2	Steering system inertia
Neuromuscular system			
J_{arm}	0.15	kgm^2	Rotational inertia
c_p	3.07	Nm s rad^{-1}	Intrinsic damping
c_a	1.95	Nm s rad^{-1}	Co-contraction damping
k_a	7.8	Nm^{-1}	Series spring
τ_n	0.025	s	Motor neuron time const
τ_a	0.015	s	Muscle activation time const
τ_m	0.05	s	Muscle mechanical time const
T_r	0.04	s	Reflex delay
k_r	6.24	Nm rad^{-1}	Reflex gain
Cognitive control			
T_c	0.2 (0.1)	s	Cognitive delay
q_1	10^3 (10^4)	m^{-2}	Weighting on lateral error
q_2	10^{-6}	rad^{-2}	Weighting on heading error
q_3	1	s^2 rad^{-2}	Weighting on steering rate

of the vehicle's centre of gravity is defined using displacements x_E and y_E in a ground-fixed coordinate system. The equations of motion for the planar vehicle dynamics are

$$m(\frac{\mathrm{d}v_Y}{\mathrm{d}t} + \omega_Z v_X) = F_{Yf} + F_{Yr} \tag{1}$$

$$I_Z \frac{\mathrm{d}\omega_Z}{\mathrm{d}t} = aF_{Y_f} - bF_{Yr} + M_Z \tag{2}$$

where F_{Yf} and F_{Yr} are the lateral forces on the front and rear axles, which are given by

$$F_{Yf} = C_f(\delta_f - (v_Y + a\omega_Z)/v_X) \tag{3}$$

$$F_{Yr} = C_r(b\omega_Z - v_Y)/v_X \tag{4}$$

where δ_f is related to the steering wheel angle δ_H by the steering ratio i_s so that $\delta_H = i_s\delta_f$. Also introduced, the front and rear axle cornering stiffnesses C_f and C_r that are set to half the values for steady cornering, to account for the reduction caused by braking force.

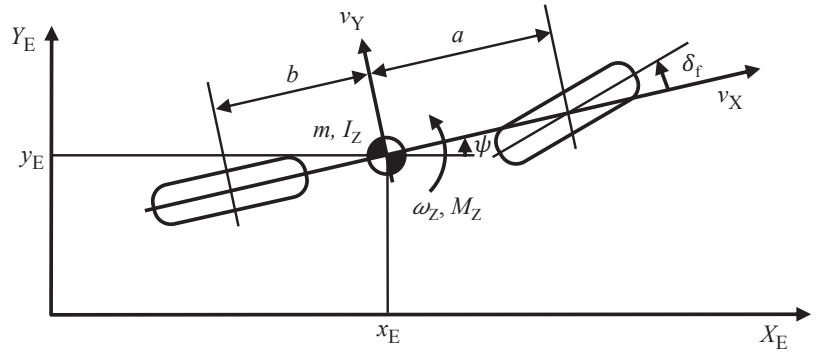

Figure 8.: Vehicle planar dynamics model seen from above.

Longitudinal vehicle speed v_X in the simulation is taken from recordings of measured speed made via a sensor on the vehicle's gearbox. A longitudinal accelerometer signal was recorded during the experiments, but unsuitable filtering meant it couldn't be used as an input to the simulation. Therefore the longitudinal vehicle acceleration $\mathrm{d}v_X/\mathrm{d}t$ has been determined by differentiating the measured speed signal. First, smoothing was performed using the Savitzky-Golay method with a 2^{nd} order polynomial and a window of 0.25 s, followed by two-point numerical differentiation. The signal was then low-pass filtered (2^{nd} order Butterworth) at 2.5 Hz.

A split-μ braking event is represented in the simulation by applying the yaw moment M_Z to the centre of gravity as

$$M_Z = -md \cdot \frac{\mathrm{d}v_X}{\mathrm{d}t} \tag{5}$$

Where d is the lateral distance from the vehicle centreline to the line of action of the total longitudinal braking force.

The vehicle planar dynamics model constitutes the block labelled $H_{vehicle}$ in Fig. 7, and inputs M_Z and v_X derived from the experimental data. The steering wheel angle δ_H is generated by the steering and driver parts of the model. Output from the vehicle block is labelled $\mathbf{x}$ and represents full state feedback of the system to the driver.

Measured and simulated responses of the vehicle undergoing automatic emergency braking with the emulated split-μ condition are shown in Fig. 9. The steering was locked so that $\delta_H = 0^o$. The top graph shows the measured speed from the experiment. The middle graph shows the measured and simulated yaw rate of the vehicle. There is broadly good agreement. The small differences are likely due to the absence of roll dynamics in the vehicle model, and due to the approximations involved in determining the yaw moment M_Z from the measured speed

signal. The bottom graph shows the measured and simulated vehicle trajectories at the centre of gravity of the vehicle. The slightly larger lateral displacements of the simulated trajectory correspond to the initially larger simulated yaw response seen in the middle graph. The difference in longitudinal distance travelled is due to discrepancies between the GPS data and the integrated speed measurement from the gearbox sensor. There is sufficiently good agreement between the measured and simulated vehicle response in the locked steering condition to proceed with adding details of the steering mechanism and the driver to the vehicle model.

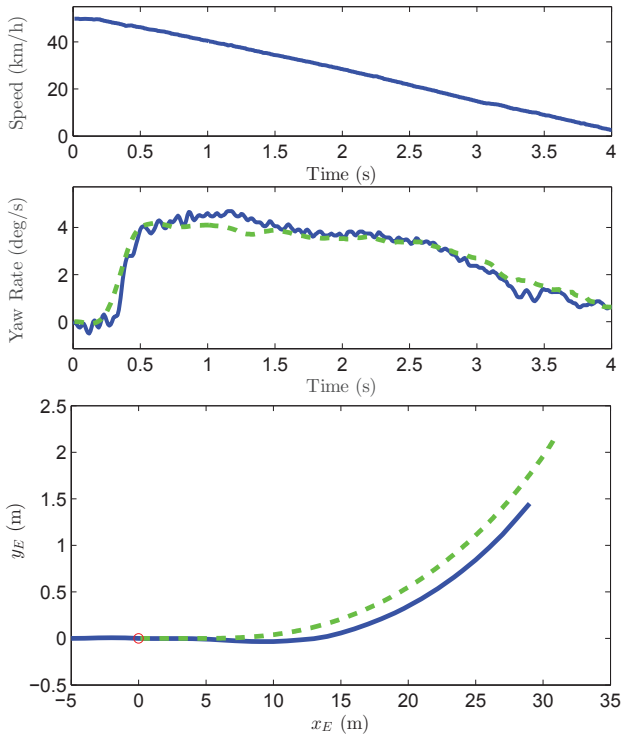

Figure 9.: One measured (blue solid) and the corresponding simulated (green dashed) responses of the test vehicle undergoing automatic emergency braking with emulated split-μ condition. Steering is locked. Top: measured vehicle speed. Middle: yaw rate. Bottom: vehicle trajectory.

4.2. *Steering System*

The steering mechanism of the vehicle is a complicated electro-mechanical-hydraulic system. Highly nonlinear mathematical models with tens of degrees of freedom and hundreds of parameters could be used to represent its behaviour precisely. For the present purpose, the simplest possible model that represents satisfactorily the torque-angle behaviour during split-mu braking is sought.

It is assumed that there is no compliance in the steering mechanism and that the torque feedback acting on the rotating steering system, $M_{vehicle}$, is the sum of the normal steering torque response, H_{feel}, and the torque disturbance, M_{offset}, caused by uneven braking forces.

The normal steering torque feedback, M_{feel}, is approximated by a parallel spring and damper, where there is some dependence on the speed of the vehicle according

to

$$M_{feel} = -(k_s \delta_H + c_s \frac{\mathrm{d}\delta_H}{\mathrm{d}t}) \sqrt{\frac{v_X}{v_{ref}}} \tag{6}$$

where k_s is the steering stiffness, c_s the steering damping and v_{ref} a reference speed.

The stiffness term in (6) represents the self-centering action of the vehicle's steering system. The damping term represents the hysteretic component of the vehicle's steering torque feedback characteristic. The use of a square root function to model the dependency of torque feedback on vehicle speed was determined by fitting to data supplied by the vehicle manufacturer. The suitability of (6) and the values used for its parameters were determined through comparison with data measured from the vehicle, as described later in this section.

The component of steering torque feedback M_{offset} arising from a non-zero steering offset, r_k, and unsymmetrical braking forces is calculated from the measured acceleration response of the test vehicle as

$$M_{offset} = -\frac{m r_f r_{split} r_k}{i_s p_s} \frac{\mathrm{d}v_X}{\mathrm{d}t} \sqrt{\frac{v_X}{v_{ref}}} \tag{7}$$

where $m\frac{\mathrm{d}v_X}{\mathrm{d}t}$ is the total braking force, r_f is the braking force on the front axle expressed as a fraction of the total braking force on the vehicle, r_{split} is the difference in left and right braking forces on the front axle expressed as a fraction of the total braking force on the front axle, and p_s the power steering torque ratio.

The resulting steering torque $M_{vehicle}$ is together with the driver torque, M_{muscle}, applied to the total inertia of the steering system, J_{steer}. The steering wheel angle can then simply be derived using Newton's second law. In this the total inertia J_{steer} includes the sum of the rotational inertias of the driver's arms, J_{arm}, and the steering system itself, J_{mech}, all referenced to the rotation axis of the hand wheel. Moreover, as pointed out earlier J_{mech} depends on the setting of r_k due to the functionality of the power steering unit.

Fig. 10 shows how the steering system model compares to experimental data, both when r_k=0 cm and r_k=12 cm. The vertical axis represents steering wheel torque, which here is defined as the torque present in the steering column just below the steering wheel[1]. In both cases agreement between measurement and simulation is thought to be sufficient for the model to aid understanding of the measured driver steering behaviour.

4.3. *Driver Model*

The mathematical model of the driver shown in Fig. 7 is closely based on that described in [18] and [23], where further details of the parameters and comparison with measured driver responses can be obtained. This driver model is particularly suitable for the present application because it represents both the neuromuscular dynamics and the cognitive control of the human driver. Many other driver models in the literature represent only cognitive control. It is important to include neuromuscular dynamics in the model because the angular response of the steering wheel to the torque disturbance on the steering wheel might be influenced by the dynamics of the driver's arms.

[1]This definition is different from that in ISO 8855, [13], due to steering wheel inertia effects

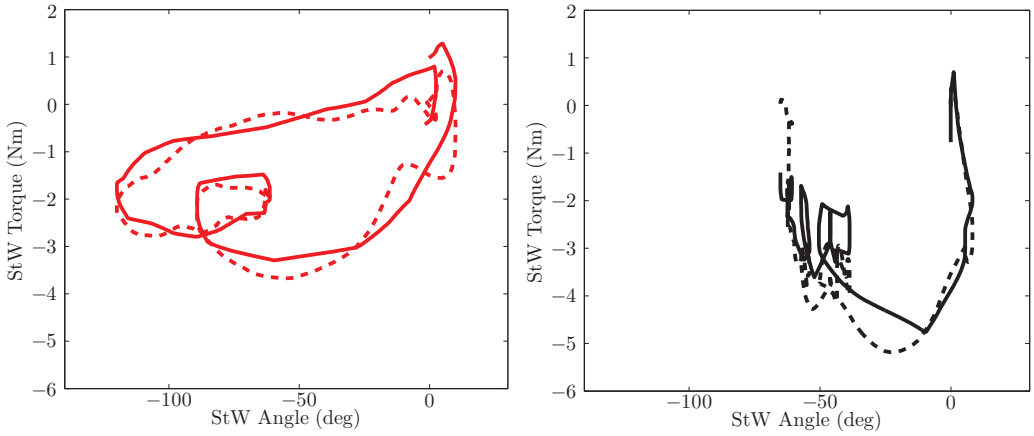

(a) r_k=0 cm. (b) r_k=12 cm.

Figure 10.: Measured (solid) and simulated (dashed) steering wheel torque against steering wheel angle for one unexpected run at 50 km/h. StW means steering wheel.

Referring to Fig. 7, the driver model is closely coupled to the vehicle model, indicated by the vertical dashed double line. The coupling takes place at the steering wheel (J_{steer}) where the steering torques from the vehicle ($M_{vehicle}$) and the driver (M_{muscle}) combine to give a resultant torque (M_{total}) acting on the rigidly connected inertias of the steering wheel and driver's arms (J_{steer}). The steering torque from the driver (M_{muscle}) is generated by the driver model, which consists of two main parts: neuromuscular and cognitive. The neuromuscular part includes the muscles (H_{act}, M_{act}, $H_{intrinsic}$, $M_{intrinsic}$) and the stretch reflex loop (H_{reflex}); these are described in more detail in section 4.3.1. The cognitive part (K, T_c, H_{fwd}) is described in section 4.3.2 and is responsible for sensing the vehicle response ($\mathbf{x}$), generating the control signals that activate the neuromuscular system (α and γ), and guiding the vehicle along the target road path ($y_{Etarget}$). The parameters of the driver model are described in the following sections; further details can be found in [18].

4.3.1. Neuromuscular

The neuromuscular system comprises the muscles and stretch reflexes that are involved in applying torque M_{muscle} to the steering inertia J_{steer}. The torque M_{muscle} is the resultant of: the torque M_{act} arising from neural activation of the muscle via the activation dynamics block H_{act}; and torque $M_{intrinsic}$ arising from the intrinsic passive properties of the muscle ($H_{intrinsic}$) activated by motion of the steering wheel, δ_H. The activation dynamics block H_{act} represents the electro-chemical processes involved in neural activation of the muscles and comprises several first order lags in series: the motor neuron time constant τ_n; the muscle activation time constant τ_a; and the mechanical time constant τ_m. The intrinsic passive properties $H_{intrinsic}$ are predominantly damping in nature, the value of which depends on the degree of muscle activation. More muscle activation means that there is more cross-linking of muscle filaments and therefore more dissipative loss when the muscle changes length. The properties are represented by a linear viscous damper c_p in parallel with a series spring-damper (k_a and c_a). The series spring-damper provides the frequency-dependent damping observed in measured data. The muscles are activated via the motor neurons in the spine by the alpha motor neuron signal α sent from the motor centre of the brain. The muscles can also be activated via the motor neurons in the spine by a stretch reflex loop, which is essentially a lo-

cal displacement feedback control H_{reflex} comprising a proportional gain k_r and a pure delay T_r arising from the neural conduction velocity. The stretch reflex loop provides some of the stiffness presented by the arms when disturbed by torque $M_{vehicle}$ from the hand wheel. The stretch reflex loop is driven by a gamma motor neuron signal γ which is essentially a hand wheel angle demand signal from the brain. See [18] for further details of these parameters and their values[1].

4.3.2. Cognitive Control

The remaining part of the driver model, that is, generation of the alpha and gamma signals, represents the driver's cognitive control action. The driver is assumed to steer the vehicle so as to minimise the lateral and heading deviation from the centre of the lane. This is expressed mathematically with a cost function as

$$J = \int \left(q_1 y_E^2 + q_2 \psi^2 + q_3 \left(\frac{\mathrm{d}\delta_H}{\mathrm{d}t} \right)^2 \right) \cdot \mathrm{d}t \tag{8}$$

where q_1, q_2, and q_3 are weighting values that specify the priority that the driver places on minimising lateral deviation y_E, heading deviation ψ, and steering wheel angular rate $\frac{\mathrm{d}\delta_H}{\mathrm{d}t}$. The full-state feedback gain K required to minimise the cost function can be derived as a linear quadratic regulator. The theoretical details are described in [18, 23], but a brief outline follows. A discrete-time state-space system comprising all the blocks in Fig. 7 except the forward model H_{fwd} and the controller K is assembled. Since the target path $y_{Etarget}$ is straight there is no additional information to be gained by looking ahead at the future target path, so the shift register and additional states provided in [18, 23] for preview of the target path are not required. The state vector of the system represents all the information given to the driver and assumes perfect full-state measurement. An optimal full-state feedback gain vector K is calculated by applying Matlab's 'lqr' function to the system, using the cost function of equation (8). The optimal alpha motor neuron control signal α is calculated by multiplying the gain vector K by the state vector $\mathbf{x}$ at each time step of the simulation. In [18, 23] the vehicle speed is treated as constant and thus the cognitive steering controller gain K is time invariant. In the present case the vehicle speed varies and there are several possibilities for modelling the driver's steering control in this case. One is to fix K for the vehicle speed at which the manoeuvre begins. This is the most straightforward approach, but might lead to unsatisfactory or unstable control as the vehicle speed reduces. A more sophisticated approach is to tune K at each time step to account for the predicted future speed variation of the vehicle. This 'variable-model prediction' was the approach taken in [24] in relation to future variation of vehicle dynamics arising from nonlinear tyres. For the present work an intermediate approach is taken; the controller K varies with vehicle speed, but at each speed the controller is optimised for that speed only. This 'gain-scheduling' approach was also taken by Sharp [25] in relation to a driver's speed control. The approach works well if the speed of the vehicle varies slowly compared to the bandwidth of the steering controller, which is thought to be a valid assumption in the present case. It is also assumed in calculating the controller K that the vehicle speed does not drop below 0.1 m s^{-1}, to avoid numerical problems.

[1]There are two typographical errors in [18]: in figure 5(b) the spring k_a and damper c_a should be exchanged, so that c_a connects to ground and k_a connects to the inertia, and in equation (5), c_a on the right hand side of the equation should be k_a.

The controller K generates the alpha motor neuron control signal α, which can be thought of as a feedforward torque command signal. The alpha signal α is subjected to a time delay T_c to represent cognitive and sensory delays. The value of this delay can vary depending on the attentiveness of the driver. The gamma motor neuron control signal γ is generated by passing the alpha signal α through a forward model H_{fwd} of the neuromuscular, steering and vehicle system. The gamma signal γ can be regarded as the expected hand wheel angle arising from applying the alpha signal α to the neuromuscular, steering and vehicle system. Any unexpected disturbances on the system, such as torque disturbance M_{offset} on the steering, cause the reflex loop to compensate for the difference between expected and actual steering wheel angles. The action of the stretch reflex loop is not subject to the cognitive delay T_c. Thus unexpected disturbances on the vehicle can be acted upon by the stretch reflex before the driver activates the muscles directly via the alpha signal α.

5. Simulation Results

The driver and vehicle model shown in Fig. 7 was used to simulate the unexpected and repeated split-μ braking experiments, with and without steering wheel disturbance. For the simulation the driver's target path was assumed to be a straight line in the centre of the lane. The measured speed was the basis of the inputs to the simulation, governing: the speed v_X of the vehicle; the yaw moment M_Z applied to the vehicle according to (5); and in the case of steering wheel disturbance, the torque M_{offset} applied to the steering wheel according to (7). The driver and vehicle model parameter values for the unexpected runs are given in Table 4. The cost function weights and cognitive time delay were iterated manually to achieve good agreement between measurement and simulation. The neuromuscular parameter values (J_{arm}, c_p, c_a, k_a, k_r) were set according to the relaxed condition reported in [18] and multiplied by 1.56 to account for the larger radius of the steering wheel in the truck (0.225 m compared to 0.18 m in [18]). The values were identified from experimental data reported in [26]; the experiments involved applying a random torque disturbance and measuring the angular response. The values of the time constants (τ_n, τ_a, τ_m, T_r) were set as reported in [18, 26]; these values were derived from information published in the neuroscience literature, reviewed in [26].

Fig. 11 shows the measured vehicle speed, and the measured and simulated steering wheel angle δ_H, steering torque M_{col} and vehicle yaw rate ω_Z. The left hand graphs correspond to the unexpected runs. The right hand graphs correspond to the repeated runs. The measured data in these graphs are averaged across all the test drivers. Averaging the repeated runs of a driver is reasonable if the variation between runs is the result of random processes. If not, then there is risk that the averaged data is not representative of the driver. In [24], data from a range of drivers repeatedly performing a transient manoeuvre was analysed statistically (normalised cross-correlation). It was found that run-to-run variation for each individual driver could be regarded as a random process. Averaging the responses across drivers is more difficult to justify since there might be systematic differences between the drivers' steering strategies. However, in the presence of limited data (as in the present case), a trade-off must be made between masking systematic variations between drivers and reducing the variance arising from random processes within the drivers.

The time development of the measured and simulated responses shown in Fig. 11 can be explained as follows. Starting with the unexpected runs in the absence of steering wheel disturbance (red lines in left hand graphs of Fig. 11) it can be

seen that the vehicle yaw rate response begins at about 0.2 s and rises significantly at about 0.3 s. The measured initial response shows some high frequency small amplitude oscillation not present in the simulation. This is likely due to the low-order vehicle model that does not include roll or pitch dynamics or tyre transient dynamics. Nevertheless the measured and simulated responses agree quite well thereafter.

There is similar agreement in the steering torque responses, with the torque building up from about 0.5 s. In the absence of steering wheel disturbance, there is no reflex action and the steering torque arises from the driver's cognitive action. The time gap from onset of vehicle yaw rate response to steering torque response is consistent with the simulated cognitive time delay T_c of 0.2 s. The cost function weight values are chosen to give good agreement of the steering angle and vehicle response over the duration of the manoeuvre. It appears from the identified values of the cost function weights that the driver places emphasis only on minimising lateral path error (q_1 =1000) compared to heading error (q_2 =10^{-6}), but in practice the two responses are kinematically related and therefore the heading error is not uncontrolled. There is some discrepancy between the measured and simulated steering angle in the later part of the manoeuvre, which might be explained by time variation of the driver's cognitive control strategy. Turning attention to the unexpected runs with steering wheel disturbance (black lines in left hand graphs) the presence of the disturbance is clearly seen in the plot of steering torque. The torque moves from zero at about 0.15 s, just before the yaw rate of the vehicle responds. Although the steering torque responses of the vehicles with and without the steering wheel disturbance are noticeably different, the yaw responses of the vehicle are very similar, which indicates that the dominant disturbance on the vehicle is the yaw moment M_Z rather than the steering wheel disturbance M_{offset}. There is discrepancy between the simulated and measured steering torque for the runs with steering wheel disturbance (black lines), despite the steering angle responses agreeing quite well. This is likely due to discrepancy in the steering model, section 4.2.

Inspecting the steering angle graph it can be seen that the steering wheel disturbance causes the steering angle to move to a positive value for a short period at about 0.5 s, reinforcing the disturbing effect of the yaw moment disturbance M_Z on the vehicle. The nature of the steering angle response up to this point is determined by the dynamic properties of the steering components and the passive and reflex properties of the driver's arms. After this point the cognitive action dominates the driver's steering. However the effect of the steering wheel disturbance appears to be small and the reason for this is discussed in the next section.

The left hand graph in Fig. 12 shows the average vehicle trajectories of measured and simulated unexpected runs, with and without steering wheel disturbance. The simulated trajectory shows the expected larger lateral displacement of the vehicle with steering wheel disturbance (black dashed line compared to red dashed line). This disagrees with the averages of the measured trajectories, however the large standard deviation of the measured trajectories means that the difference in the measured averages is not significant. Considering the repeated runs shown in the right hand side of Fig. 11, it is immediately noticeable that the drivers' responses to repeats of the braking event occur earlier than for the unexpected event. This is accounted for in the simulation by reducing the cognitive time delay T_c from 0.2 s to 0.1 s. Another difference is that the steering action appears to be faster. This is accounted for in the simulation by increasing the cost function weighting on lateral path error by a factor of 10 to q_1 =10^4. These changes to the simulated driver's cognitive response time and control strategy are consistent with the test drivers

having recent experience of the braking event and anticipating further events. No other changes were made to the driver or vehicle parameter values given in Table 4. As with the unexpected runs, the simulation indicates that the steering wheel disturbance makes a negligible contribution to the driver's steering response. Fig. 12 shows that the simulated vehicle trajectories correctly predict the reduction in lateral path error for the repeated runs compared to the unexpected runs.

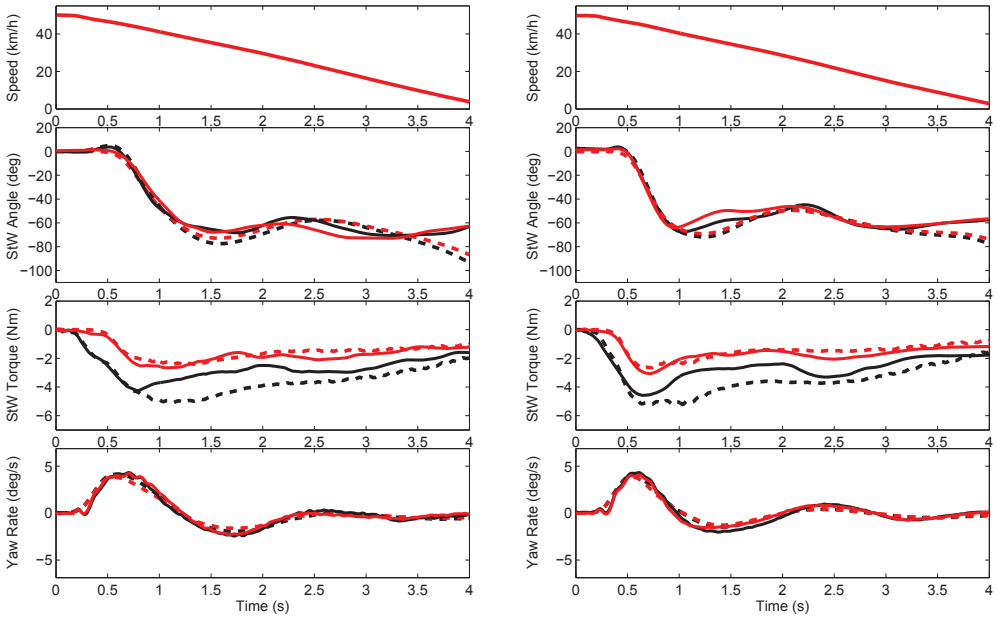

(a) Unexpected runs. (b) Repeated runs.

Figure 11.: Measured and simulated time series at initial speed 50 km/h. Red lines correspond to runs without steering wheel disturbance. Black lines correspond to runs with steering wheel disturbance. Solid lines are averaged measured data. Dashed lines are simulation. StW means steering wheel.

6. Discussion

The measured data strongly indicate that the steering wheel disturbance during the split-μ braking event had negligible influence on the average maximum lateral displacement of the vehicle, particularly compared to the effect of the yaw moment on the vehicle. The small influence of the steering wheel disturbance can also be seen in the average maximum positive steering wheel angle, which is only about 4^o at 0.5 s as shown in Fig. 11(a). In contrast, other studies of driver response to steering torque disturbances have shown a significant effect, particularly from the stretch reflex [27]. Therefore it is of interest to use the driver model to explain the apparently small influence of the steering wheel disturbance (corresponding to M_{offset} in the model, Fig. 7). Interrogation of the experiment and simulation data reveals that the torque M_{offset} applied to the neuromuscular and steering system rises from near zero at 0.2 s to around 2.5 Nm at 0.4 s, a rise time of 0.2 s. The rate of torque increase is influenced by the brake system dynamics, tyre relaxation dynamics and steering gear dynamics. The torque applied to the steering wheel by cognitive action (via the alpha signal α) begins at about 0.4 s. Thus the steering wheel torque M_{offset} is applied for only 0.2 s before the cognitive action begins. The

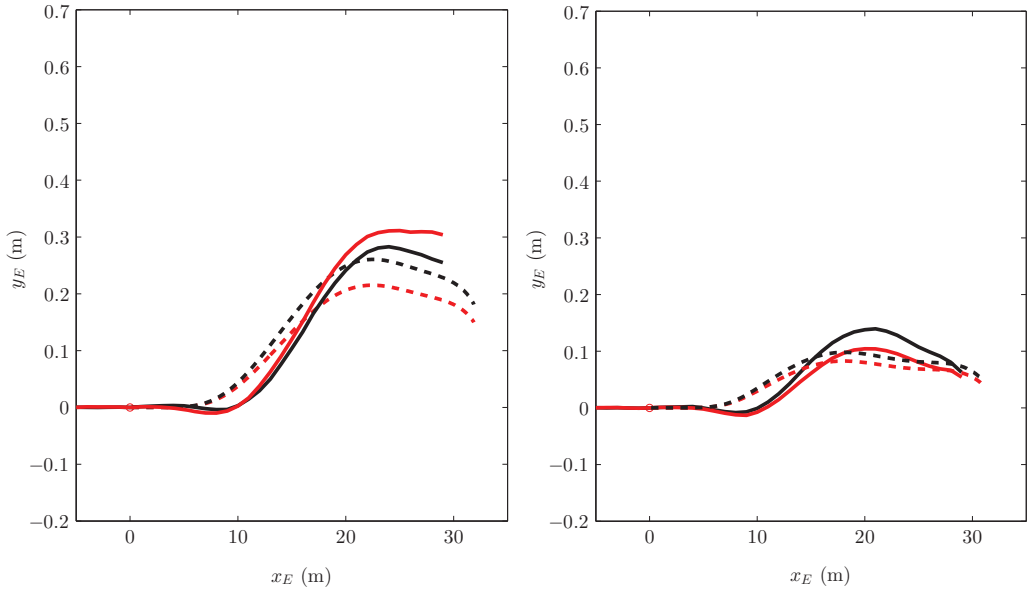

(a) Unexpected runs.

(b) Repeated runs.

Figure 12.: Measured and simulated trajectories at initial speed 50 km/h. Red lines correspond to runs without steering wheel disturbance. Black lines correspond to runs with steering wheel disturbance. Solid lines are averaged measured data. Dashed lines are simulation.

angle response of the steering wheel during this time is determined predominantly by the passive and reflex properties of the neuromuscular and steering system. The reflex gain k_r has a relatively small influence because it is only one of several influential parameters in this system, the others being the intrinsic stiffness (k_a) and damping (c_a and c_p) of the muscles, the steering stiffness (k_s) and damping (c_s), and the inertia of the neuromuscular and steering system (J_{steer}). If the neuromuscular and steering system is approximated as a 2^{nd} order mass-spring-damper system, the natural frequency is about 1 Hz with a damping ratio of 2 and stiffness 7.74 Nm/rad. The angle response of this overdamped 2^{nd} order system to a step input torque of 2.5 Nm is only 4^o after 0.2 s, which is consistent with the averaged measured angle. In summary the small effect of the steering wheel disturbance and the small influence of the reflex gain can be attributed mainly to: (i) the time taken for the steering wheel disturbance torque to build up; (ii) the slow response characteristics of the neuromuscular and steering system.

Further insight to the reflex action in this scenario can be obtained by increasing the reflex gain by a factor of 5 and keeping all other parameter values in the driver-vehicle model unchanged. The result is only a slight reduction in maximum lateral displacement of the vehicle for the case with steering wheel disturbance (from 0.261 m to 0.252 m), which is consistent with the preceding argument. The role of the intrinsic muscle dynamics on the response to the steering wheel disturbance can be estimated by running the simulation with the intrinsic stiffness and damping parameters set to zero throughout the run (for completeness the reflex gain is also set to zero, but as has been shown it has only a small influence). The cognitive action takes place as normal after the passage of the cognitive delay. In this case the maximum lateral displacement of the vehicle increases from 0.261 m to 0.359 m. This can be regarded as an upper bound on the lateral displacement arising from the driver maintaining hold of the steering wheel but with completely

relaxed muscles. Perhaps the most significant parameter in determining the vehicle response before the cognitive action begins is the cognitive time delay. Increasing the delay from 0.2 s to 1.0 s increases the maximum lateral vehicle displacement from 0.261 m to 0.940 m.

The measured data also revealed that the maximum lateral displacement of the vehicle was reduced in the repeated (expected) runs. In the simulation the drivers' response to the repeated runs was represented by shortening the cognitive time delay from 0.2 s to 0.1 s and increasing the weight on lateral path error by a factor of 10. In the experiment it is possible that the drivers were able to learn the steering control action necessary to compensate the yaw moment disturbance and thus operate in a feedforward (open loop) manner, rather than feedback (closed loop). It should also be noted that the repeated runs in the experiment were all in the same direction as the initial unexpected run, which might allow a shorter cognitive time delay than if the driver had to perceive the direction of the disturbance. Extending the model to allow for a change in control action from closed loop to predominantly open loop might provide a better representation of the measured response in the repeated runs.

In terms of improving the vehicle to reduce maximum lateral deviation in a split-μ braking event, a natural next step would be to start guiding the driver with a stabilising steering wheel torque. The consequences of this are not obvious, but the driver model could be used also in this case to underpin understanding [28].

7. Conclusion

An experiment has been performed with 24 subjects, driving an instrumented tractor unit, to determine the effect of a destabilising steering wheel torque during an automatic split-μ braking event. In the initial unexpected exposure half of the subjects ran with steering wheel disturbance (arising from positive kingpin offset), and half ran without (no kingpin offset). No significant difference, originating from the disturbance, was observed between the two groups in any of the analysed metrics. This finding contrasts with that in [16] where positive kingpin offset was found to cause an increase in lateral vehicle deviation during a simulated tyre blow out event. The lateral deviations of the vehicle in the split-μ braking events were up to 0.6 m, but the average deviation was reduced in repeated runs. Both in the initial unexpected exposure runs and in the repeated runs a vague overshoot in steering wheel angle, at around 0.2 s after the vehicle started yawing, was noted when steering wheel disturbance was present. However when considering the relative amplitude it is estimated to have a practically insignificant effect on the path of the vehicle. These findings add substantially to those reported in [8].

A review of the published literature revealed that the scenario of a heavy truck in AEBS split-μ events appears not to have been simulated using a detailed driver model. An existing driver and vehicle model [18] was adapted to simulate the split-μ braking experiment. The vehicle model was found to predict the locked steering response of the test vehicle satisfactorily; further improvement might be obtained by more detailed modelling of the transient dynamics of the vehicle in the first part of the manoeuvre. The driver-vehicle model was found to predict the measured responses satisfactorily. The model predicted that the steering wheel disturbance causes a small increase in lateral path error, due to the effect on steering angle reinforcing the yaw moment disturbance on the vehicle. However, the model indicated that the muscle stretch reflex action contributes negligibly to the driver's response to the steering wheel disturbance, compared to the influence of the intrinsic muscle properties. The cognitive time delay was found to have a significant effect on the

maximum lateral deviation of the vehicle, with or without a steering wheel disturbance. The driver's response to repetitions of the braking event was simulated by reducing cognitive delay by 0.1 s and increasing the weight on lateral path error by a factor of 10. However it was noted that in practice the driver might employ some degree of feedforward control in repeated events, rather than the purely feedback control represented by the model.

8. Acknowledgements

The authors would like to thank Chalmers Area of Advance Transport for financing an exchange that enabled this cooperation.

References

[1] C. Grover, I. Knight, F. Okoro, I. Simmons, G. Couper, P. Massie, and B. Smith, *Automated emergency brake systems: Technical requirements, costs and benefits*, Published project report PPR 227, TRL Limited, 2008.
[2] J. Strandroth, M. Rizzi, A. Kullgren, and C. Tingvall, *Head-on collisions between passenger cars and heavy goods vehicles: Injury risk functions and benefits of autonomous emergency braking*, in *Proceedings of the IRCOBI Conference*, 2012.
[3] European Union, Commission regulation (EU) No 347/2012 of April 2012; (2012), .
[4] F. Vlk, *Handling performance of truck–trailer vehicles: A state–of–the–art survey*, International Journal of Vehicle Design 6 (1985), pp. 323–361.
[5] ECE, UN Vehicle regulations - 1958 Agreement, Addendum 12: Regulation No. 13, Revision 7; (2011), .
[6] G. Morrison and D. Cebon, *Model-Based Stabilization of Articulated Heavy Vehicles under Simultaneous Braking and Steering*, in *Proceedings of the 12th International Symposium on Advanced Vehicle Control*, 2014.
[7] S.W. Zhou, S.Q. Zhang, and G.Y. Zhao, *Jackknife control on tractor semi-trailer during emergency braking*, Advanced Materials Research 299 (2011), pp. 1303–1306.
[8] K. Tagesson, B. Jacobson, and L. Laine, *Driver response to automatic braking under split friction conditions*, in *Proceedings of the 12th International Symposium on Advanced Vehicle Control*, 2014.
[9] K. Tagesson, L. Laine, and B. Jacobson, *Combining coordination of motion actuators with driver steering interaction*, Traffic injury prevention 16 (2015), pp. S18–S24.
[10] S. Kharrazi, M. Lidberg, P. Lingman, J.I. Svensson, and N. Dela, *The effectiveness of rear axle steering on the yaw stability and responsiveness of a heavy truck*, Vehicle System Dynamics 46 (2008), pp. 365–372.
[11] Volvo Trucks, Volvo Dynamic Steering a breakthrough for effortless steering without strain or pain; Press information (2013), .
[12] ZF, ZF Steering Systems Unveils Energy Saving High-Tech Solutions for the Commercial Vehicle Segment; Press Information (2012), .
[13] ISO, *Road vehicles – Vehicle dynamics and road-holding ability – Vocabulary*, ISO 8855:2011, International Organization for Standardization, 2011.
[14] T.D. Gillespie *Fundamentals of vehicle dynamics*, Vol. 400, Society of Automotive Engineers Warrendale, PA, 1992.
[15] W. Milliken and D. Milliken, *Race car dynamics*, SAE, Warrendale (1995).
[16] K. Tagesson, B. Jacobson, and L. Laine, *Driver response at tyre blow-out in heavy vehicles & the importance of scrub radius*, in *Intelligent Vehicles Symposium Proceedings, 2014 IEEE*, 2014, pp. 1157–1162.
[17] J.P. Switkes, J.C. Gerdes, G.F. Schmidt, and M. Kiss, *Driver response to steering torque disturbances: A user study on assisted lanekeeping*, in *Advances in Automotive Control*, Vol. 5, 2007, pp. 243–250.
[18] D.J. Cole, *A path-following driver–vehicle model with neuromuscular dynamics, including measured and simulated responses to a step in steering angle overlay*, Vehicle System Dynamics 50 (2012), pp. 573–596.
[19] K. Tagesson, B. Jacobson, and L. Laine, *The influence of steering wheel size when tuning power assistance*, International Journal of Heavy Vehicle Systems 21 (2014), pp. 295–309.
[20] Q. Cheng, A study of truck driver deceleration initiation behaviour; Master's thesis, Chalmers University of Technology (2012), .
[21] TYA, *Rekrytering av lastbilsförare 2013*, , Transportfackens yrkes- och arbetsmiljönämnd, 2013.
[22] S. Kharrazi, *Steering based lateral performance control of long heavy vehicle combinations*, PhD thesis, Chalmers University of Technology, 2012.
[23] D. Cole, A. Pick, and A. Odhams, *Predictive and linear quadratic methods for potential application to modelling driver steering control*, Vehicle System Dynamics 44 (2006), pp. 259–284.
[24] S.D. Keen and D.J. Cole, *Application of time-variant predictive control to modelling driver steering skill*, Vehicle System Dynamics 49 (2011), pp. 527–559.
[25] R. Sharp, *Application of optimal preview control to speed-tracking of road vehicles*, Proceedings of the

Institution of Mechanical Engineers, Part C: Journal of Mechanical Engineering Science 221 (2007), pp. 1571–1578.
[26] W. Hoult, *A neuromuscular model for simulating driver steering torque*, PhD thesis, University of Cambridge, 2009.
[27] A. Kullack, I. Ehrenpfordt, K. Lemmer, and F. Eggert, *ReflektAS: lane departure prevention system based on behavioural control*, IET Intelligent Transport Systems 2 (2008), pp. 285–293.
[28] X. Na and D.J. Cole, *Game-Theoretic Modeling of the Steering Interaction Between a Human Driver and a Vehicle Collision Avoidance Controller*, Human-Machine Systems, IEEE Transactions on 45 (2015), pp. 25–38.

9. Appendix

Table 5.: Overview of driver attributes and number of completed valid runs. The first column lists run type. The second column tells whether a steering wheel, StW, torque disturbance was active or not. The first eight rows provide details about driver id, age, gender (M means male and F means female), and group membership. The remaining rows contain the number of completed valid runs performed by each driver. In the case where a run is classified as invalid a letter indicates the cause. In case the driver pressed the accelerator pedal during the first 3.5 s the letter a is used. In case the driver pressed the brake pedal during the first 3.5 s the letter b is used. In the case where the measurement failed due to missing signals or that the test instructor missed a run the letter m is used. As an example the coding 1^{ab} means that one run is considered as valid and two are classified as invalid since the driver pressed the accelerator pedal in one and the brake pedal in the other. The GPS sensor and the steering wheel torque sensor stopped functioning in some runs; this was the most common reason for measurement failure. Moreover, heavy rain interrupted many of the runs with driver 24, which is why there are many m's in this column.

		Driver ID																						
		1	**2**	**3**	**4**	**5**	**6**	**7**	**8**	**9**	**10**	**11**	**12**	**13**	**14**	**15**	**16**	**17**	**18**	**19**	**20**	**21**	**22**	**23**	**24**
		Age																							
		53	30	27	54	29	29	28	54	51	30	48	47	63	60	57	60	53	46	36	41	33	31	53	27
		Gender																							
		M	F	M	M	M	M	M	M	M	F	M	M	M	M	M	M	M	M	M	M	F	M	M	M
		Group																							
		B	B	A	B	A	B	A	B	A	B	A	B	B	A	B	A	A	A	B	A	B	A	B	A
Run	**StW disturbance**	**Number of completed valid runs**																							
Unexpected, 50 km/h	Yes	0	0	1	0	0^{a}	0	0^{a}	0	1	0	1	0	0	1	0	1	1	1	0	1	0	1	0	1
Unexpected, 50 km/h	No	0^{b}	1	0	1	0	1	0	1	0	0^{b}	0	1	1	0	1	0	0	0	1	0	1	0	1	0
Repeated, 50 km/h	Yes	1^{mm}	3	0^{bbm}	3	0^{amm}	3	0^{bmm}	0^{aam}	2^{m}	0^{bbb}	2^{m}	0^{bbb}	1^{bb}	1^{mm}	0^{bbm}	3	2^{m}	2^{m}	2^{b}	2^{m}	2^{m}	2^{m}	1^{mm}	1^{mm}
Repeated, 50 km/h	No	1^{mm}	2^{m}	0^{bbb}	2^{m}	1^{am}	2^{m}	0^{mmm}	2^{m}	2^{m}	0^{abm}	3	1^{bm}	1^{bm}	3	2^{m}	3	3	3	2^{m}	3	1^{bm}	1^{am}	2^{m}	0^{mmm}
Repeated, 70 km/h	Yes	1	1	0^{b}	1	1	1	1	0^{a}	1	0^{b}	1	0^{b}	1	1	0^{b}	1^{a}	1	1	0^{b}	1	1	1	1	0^{m}
Repeated, 70 km/h	No	0^{m}	1	0^{b}	1	1	1	1	0^{a}	1	0^{b}	1	0^{b}	1^{b}	1	0^{a}	0^{m}	1	1	0^{b}	1	1	1	0^{m}	0^{m}